



OPEN Phosphorylation of SNW1 protein associated with equine melanocytic neoplasm identified in serum and feces

Ruethaiwan Vinijkumthorn¹, Amornthep Kingkaw²,
Petchpailin Yanyongsirikarn³, Narumon Phaonakrop⁴, Sittiruk Roytrakul⁴,
Wanwipa Vongsangnak^{5,6} & Parichart Tesena¹✉

Equine melanocytic neoplasm (EMN) represents a form of skin tumor observed predominantly in grey horses aged over 15 years. Despite its prevalence, current therapeutic and preventive strategies for EMN have been subject to limited investigation. This study endeavors to shed light on potential phosphoproteins present in equine serum and fecal samples, potentially linked to EMN, with a specific focus on functional interactions in EMN pathogenesis. We examined 50 samples (25 serum, 25 feces), divided into three groups based on EMN severity: normal ($n = 16$), mild ($n = 18$), and severe EMN ($n = 16$). Equine phosphoproteome analysis identified 2,359 annotated serum phosphoproteins and 2002 annotated fecal phosphoproteins through differentially expressed proteins (DEPs). KEGG analysis emphasized the role of environmental information processing. Notably, the integrin NF-kappaB binding P-TEFb to stimulate transcriptional elongation signaling pathway, involving SNW1 protein, was implicated in early stage of EMN development in both serum and fecal samples. This highlights SNW1's potential role in mediating transcriptional processes, offering a novel marker within environmental information processing. This study enhances understanding of EMN mechanisms in horses, suggesting early detection through non-invasive methods and identifying a functional pathway involving SNW1, which could inform future treatment and prevention strategies.

Keywords Equine melanocytic neoplasm, Phosphoproteomic, Phosphorylation, SNW domain-containing protein 1

Equine melanocytic neoplasm (EMN) poses a significant concern for grey horse owners and equine practitioners due to its impact on horse health and potential economic losses¹. Typically, EMNs manifest as small single or multiple nodules on areas, such as the perineum, tail base, external genitalia, and anus, initially noticed by horse owners. While these nodules may initially remain benign, they can gradually grow over time, leading to complications and difficulties with defecation and ulceration². The predominant types of EMN in grey horses include dermal melanoma and dermal melanomatosis³.

However, conventional diagnostic methods e.g., fine needle aspiration cytology and biopsy, though invasive, fail to histologically differentiate between these types³. The recent study⁴ has demonstrated the potential of non-invasive techniques, utilizing mammalian proteome databases to detect melanoma-related proteins in equine feces and serum. Phosphoproteomics, known for its ability to delineate signaling pathways underlying various pathological conditions, including cancers, emerges as a powerful tool. This method focuses on protein phosphorylation sites, which often regulate signaling networks involved in cell proliferation, migration,

¹Department of Clinical Science and Public Health, Faculty of Veterinary Science, Mahidol University, Salaya, Puttamonthon, Nakhon Pathom 73170, Thailand. ²Interdisciplinary Graduate Program in Bioscience, Faculty of Science, Kasetsart University, Bangkok 10900, Thailand. ³Prasuarthon Small Animal Hospital, Faculty of Veterinary Science, Equine Clinic, Mahidol University, Salaya, Puttamonthon, Nakhon Pathom 73170, Thailand. ⁴Functional Proteomics Technology Laboratory, National Center for Genetic Engineering and Biotechnology, National Science and Technology Development Agency, Pathum Thani 12120, Thailand. ⁵Department of Zoology, Faculty of Science, Kasetsart University, Bangkok 10900, Thailand. ⁶Omics Center for Agriculture, Bioresources, Food, and Health, Kasetsart University (OmiKU), Bangkok 10900, Thailand. ✉email: wanwipa.v@ku.ac.th; parichart.tes@mahidol.edu

EMN groups	Median age (years), range (years)	Sex	Breed	EMN location
Normal grade 0 (<i>n</i> = 8)	15	Mare (<i>n</i> = 6) Gelding (<i>n</i> = 2)	Lusitano (<i>n</i> = 6) Pony (<i>n</i> = 2)	None
Mild grade 1 (<i>n</i> = 9)	20	Mare (<i>n</i> = 6) Gelding (<i>n</i> = 3)	Lusitano (<i>n</i> = 8) Pony (<i>n</i> = 1)	Base of the tail (<i>n</i> = 9)
Severe grade 2 (<i>n</i> = 6) grade 3 (<i>n</i> = 2)	23	Mare (<i>n</i> = 3) Gelding (<i>n</i> = 2) Stallion (<i>n</i> = 1) Mare (<i>n</i> = 2)	Lusitano (<i>n</i> = 2) TB (<i>n</i> = 2) Pony (<i>n</i> = 2) Lusitano (<i>n</i> = 1) Pony (<i>n</i> = 1)	Base of the tail (<i>n</i> = 6), peri-anal (<i>n</i> = 6) and vulva (<i>n</i> = 2) Base of the tail, peri-anal and vulva (<i>n</i> = 2)

Table 1. Signalments, clinical classification and EMN category of grey horses.

Phosphoprotein annotation	Serum			Feces				
	Number of Phosphoproteins	Total spectral counts (spectral counts per sample)			Number of phosphoproteins	Total spectral counts (spectral counts per sample)		
Normal		Mild	Severe	Normal		Mild	Severe	
Annotated phosphoproteins	2359	2402	2088	1904	2002	2038	1843	1310
Unannotated phosphoproteins	48	61	42	54	48	55	46	31
Total	2407	2463	2130	1958	2050	2093	1889	1341

Table 2. Assigned the number of phosphoproteins and total spectral counts.

metabolic regulation, and systemic inflammation⁵. While phosphoproteomics has been extensively studied in human melanoma, its application in EMN remains unexplored.

This study therefore aims to investigate candidate phosphoproteins associated with EMN in both serum and fecal samples with overall goal for identifying the key functional interactions driving EMN development. Initially, phosphoproteins were extracted from these samples and analyzed using Liquid Chromatography-Tandem Mass Spectrometry (LC-MS/MS). Subsequent data analysis involved employing various bioinformatics tools and databases for protein quantitation and identification. Functional analysis was also conducted to detect early EMN markers and associated pathways. Ultimately, the study unveils putative phosphoproteins associated with each stage of EMN and their functional interactions in equine melanoma.

Results

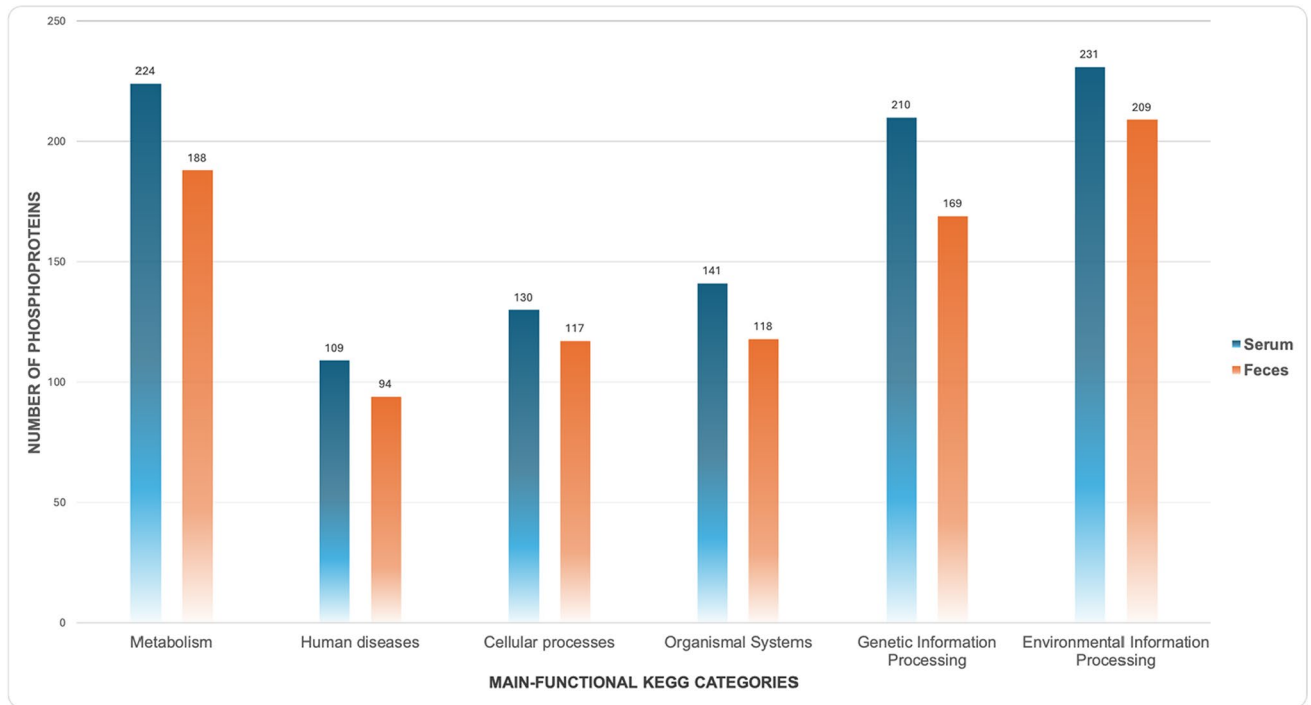
Following the EMN lesion scoring system established⁶, a group of 25 grey horses underwent classification based on the severity of their EMN lesions. The animals were stratified into normal (grade 0), mild EMN (grade 1), and severe EMN (grades 2–4) categories, taking into consideration lesion location and signalments. The signalments, clinical classification and EMN category of grey horses as shown in Supplementary file 1. In addition, Table 1 illustrates the clinical classification of EMN in grey horses, with lesions predominantly observed in older horses, occurring at a median age of 20 years for mild EMN and 23 years for severe EMN, compared to younger horses aged 15 years old. Our study delved into phosphoprotein analysis using 50 samples from grey horses, resulting in the identification of 2407 phosphoproteins in serum samples and 2050 in fecal samples. Phosphoprotein levels were quantified using individual mass spectral counts, yielding 6,551 spectral counts from serum samples and 5,323 from fecal samples. Upon dividing the serum samples into groups based on disease severity, spectral counts per sample varied across normal (2463 spectral counts), mild EMN (2130 spectral counts), and severe stages (1958 spectral counts). Similarly, for fecal samples, spectral counts per sample varied among normal (2,093 spectral counts), mild EMN (1,889 spectral counts), and severe stages (1341 spectral counts), as presented in Table 2.

The EMN lesion scoring system based on the report of the previous study⁶ composed with grade 0: free of melanoma, grade 1: the early stage the nodule 0.5 cm diameter, grade 2: several nodules with 0.5–2 cm diameter, grade 3: One or several nodules with 5 cm diameter, grade 4: Extensive confluent melanoma cover with skin; signs of destruction (necrosis, ulceration) metastasis and grade 5: Exophytic growth of tumor with the metastasis.

The annotated functions phosphoprotein profiles

The dataset comprises 2359 phosphoproteins annotated in serum samples and 2,002 phosphoproteins annotated in fecal samples. These phosphoproteins can be classified into six categories based on the KEGG database, specifically metabolism, environmental information processing, genetic information processing, cellular processes, human diseases, and organismal systems. Figure 1A presents the functional annotation analysis results for the grey horses in three different groups: those without nodule of EMN and the EMN groups with early or mild and severe stages. The dataset presents the distribution of phosphoproteins in serum and feces samples, categorized based on the main functional KEGG categories. Three severity levels were considered for each sample type, including normal, mild, and severe conditions. In terms of overall functional categories, we observed that the environmental information processing category was prominently represented in both serum and feces, with 231 and 209 identified phosphoproteins that plays a significant role in shaping the phosphoprotein landscape,

(A)



(B)

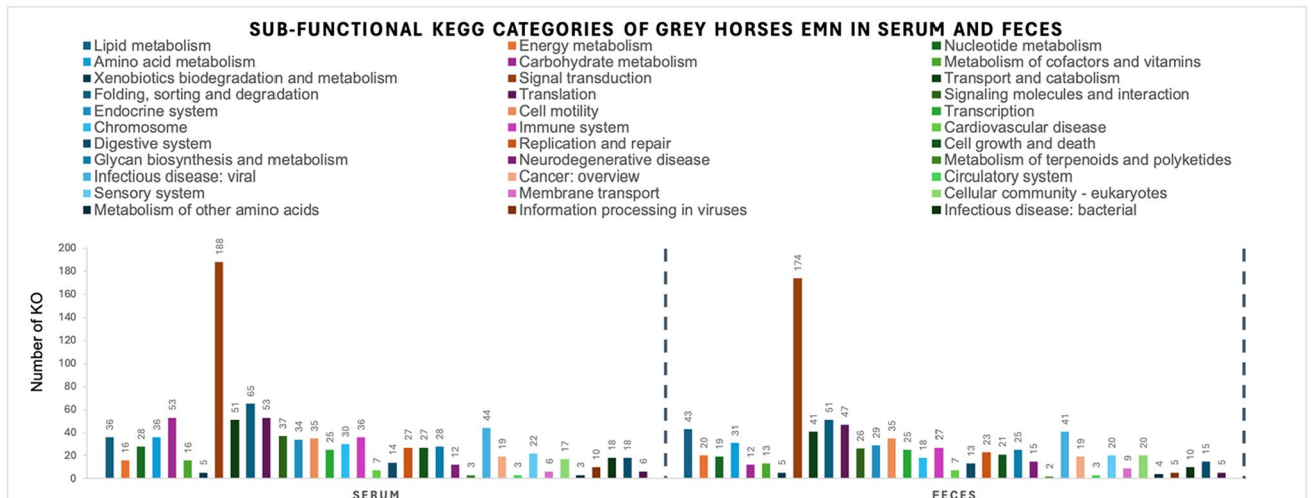


Fig. 1. Functional categories datasets of grey horses EMN in serum and feces (A) Main-functional KEGG categories (B) Sub-functional KEGG categories.

respectively. Metabolism was another robustly characterized category, with 224 phosphoproteins detected in serum and 188 in feces. Interestingly, proteins associated with human diseases were present in both serum 109 phosphoproteins and feces 94 phosphoproteins. Additionally, cellular processes were well-represented, with 130 phosphoproteins in serum and 117 in feces. While organismal systems and genetic information processing categories exhibited moderate representation in both sample types.

To analyze the sub-functional KEGG categories in serum and feces samples, we observed varied distributions across multiple metabolic pathways. Notably, lipid metabolism and energy metabolism displayed substantial representation in both serum (36 and 16, respectively) and feces (43 and 20, respectively). Amino acid metabolism and carbohydrate metabolism were also prominent categories, with 36 and 53 proteins identified in serum and 31 and 12 in feces, respectively. Signal transduction emerged as a highly represented category in both sample types, with 188 proteins in serum and 174 in feces. Other notable categories included folding, sorting, and degradation, as well as translation, with 65 and 53 proteins in serum, and 51 and 47 in feces, respectively. These

findings highlight the diverse metabolic pathways and cellular processes present in serum and feces samples, underscoring the complexity of biological systems. Further details on the sub-functional categories can be found in Fig. 1B. List of main-functional and sub-function KEGG categories of grey horses EMN in serum and feces as shown in Supplementary file 2.

Analysis of differentially expressed proteins and functional annotation of grey horses across EMN stages

To identify differentially expressed phosphoproteins (DEPs), we conducted DEP analysis on all 2359 serum annotated phosphoproteins and 2002 fecal annotated phosphoproteins using the DESeq2. From this analysis, we identified a list of 108 significant phosphoproteins in serum samples and 81 significant phosphoproteins in fecal samples with p -adjust value < 0.05 .

In our study, we analyzed a total of 113 serum phosphoproteins and 82 fecal phosphoproteins to identify putative phosphoproteins associated with EMN severity stages. For ease of analysis, we decided to normalize the intensity of the samples and normalize the values according to each horse. This allowed us to account for individual variations between horses and minimize the impact of any potential outliers. We employed all putative phosphoproteins identified in two groups of serum phosphoproteins and two groups of fecal phosphoproteins to display the differences between phosphoprotein ID lists from various differential analyses. After performing DEP analysis, we identified 48 putative phosphoproteins were expressed in the N-M group of serum phosphoproteins, while 65 putative phosphoproteins were expressed in the N-S group of serum phosphoproteins. Similarly, we found 55 putative phosphoproteins in the N-M group of fecal phosphoproteins and 27 putative phosphoproteins in the N-S group of fecal phosphoproteins, as detailed in Supplementary 3 and 4, respectively.

All of significant phosphoproteins were performed venn diagram to identify the unique phosphoproteins ID. As shown in Fig. 2, this approach provided a comprehensive overview of the phosphoprotein expression patterns and highlighted a single putative phosphoprotein, SNW domain-containing protein 1 (SNW1), which was found to be expressed in both N-M of serum and N-M of fecal. In addition, G protein subunit alpha transducin 1 (GNAT1) was found in fecal sample both of N-M and N-S stages. There were 3 phosphoproteins can be found in fecal sample in N-M and serum sample in N-S stages composed with kinesin-like protein (KIF5B), protein phosphatase 4 regulatory subunit 3B (PPP4R3B) and zinc finger protein 283 (ZNF283). Moreover, there were 5 phosphoproteins can be found both of serum N-M and serum N-S stages consist of Forkhead box protein N3 (FOXN3), NADH-ubiquinone oxidoreductase 75 kDa subunit, mitochondrial (NDUFS1), Ribokinase-like protein, Bax inhibitor 1 (TMBIM6) and ETS variant transcription factor 2 (ETV2), as shown in Table 3.

Additionally, Fig. 3 demonstrated a visual representation of the various groups categorized according to the statistically significant findings pertaining to the comparative protein expression levels (PELs).

Identifying putative protein, potential metabolic function and associated routes involved in EMN using integrative analysis

To identify putative protein, the results obtained from phosphoproteomic and proteomic data of serum and feces samples were integrated. Focusing on EMN, we found 4 putative proteins involved in EMN: ALK; Tyrosine-protein kinase receptor, ROCK1; Rho-associated protein kinase from serum samples and DGKA; diacylglycerol kinase alpha, DGKB; diacylglycerol kinase beta, from fecal samples. The results of searching the putative proteins on STITCH database are shown in Fig. 4. The comprehensive phosphoprotein expression pattern revealed notable phosphoproteins such as SNW1; SNW domain-containing protein 1, GNAT1; G protein subunit alpha transducin 1, KIF5B; kinesin-like protein, FOXN3; Forkhead box protein N3, NDUFS1; NADH-ubiquinone oxidoreductase 75 kDa subunit, mitochondrial, ETV2; ETS variant transcription factor 2, ALK; Tyrosine-protein kinase receptor, diacylglycerol kinase (DGKA, DGKB), ROCK1; Rho-associated protein kinase, SNW1; SNW domain-containing protein 1, MgADP; magnesium-adenosine diphosphate, MgATP; magnesium-adenosine triphosphate and MAGED2; melanoma antigen family D2 in *Equus caballus* that computational prediction between organism and interaction aggregated by the Stitch program.

Discussion

Diagnosing the progression of equine melanocytic neoplasm (EMN) is crucial, as this benign skin tumor commonly affects older grey horses. Despite its typically benign nature, EMN progression has been noted in around 80% of older grey horses^{2-4,13}. Early stages of EMN may go unnoticed due to the small size of the tumor, highlighting the importance of closely monitoring and managing this condition from its onset. The previous study has classified cutaneous melanocytic tumors into four forms³, with dermal melanoma and dermal melanomatosis being the most prevalent among grey horses. While benign dermal melanoma can often be surgically removed, dermal melanomatosis is incurable and associated with visceral metastasis^{2,3}. Despite the inability to histologically distinguish discrete dermal melanoma from dermal melanomatosis, their distinct clinical manifestations suggest a continuum between the two conditions^{2,3}. Early detection of discrete dermal melanoma may potentially halt the progression to inevitable dermal melanomatosis, underscoring the importance of regular monitoring by horse owners and prompt veterinary intervention. Additionally, this study represents the first application of phosphoproteomic techniques to identify and differentiate EMN stages using distinct phosphoproteins in horses. Research indicates a correlation between the progression of melanoma tumors and elder grey horses³. Our study observed mild EMN occurring in older horses at a median age of 20 years, with severe EMN appearing at a median age of 23 years. Evidence suggests a direct link between lipid metabolism in aging grey horses and melanoma tumor progression^{4,14}. While changes in lipid metabolism may contribute to the development and progression of certain cancers in humans and animals, further investigation is needed to ascertain the specific role of lipid metabolism in equine melanoma tumors and determine whether age-related

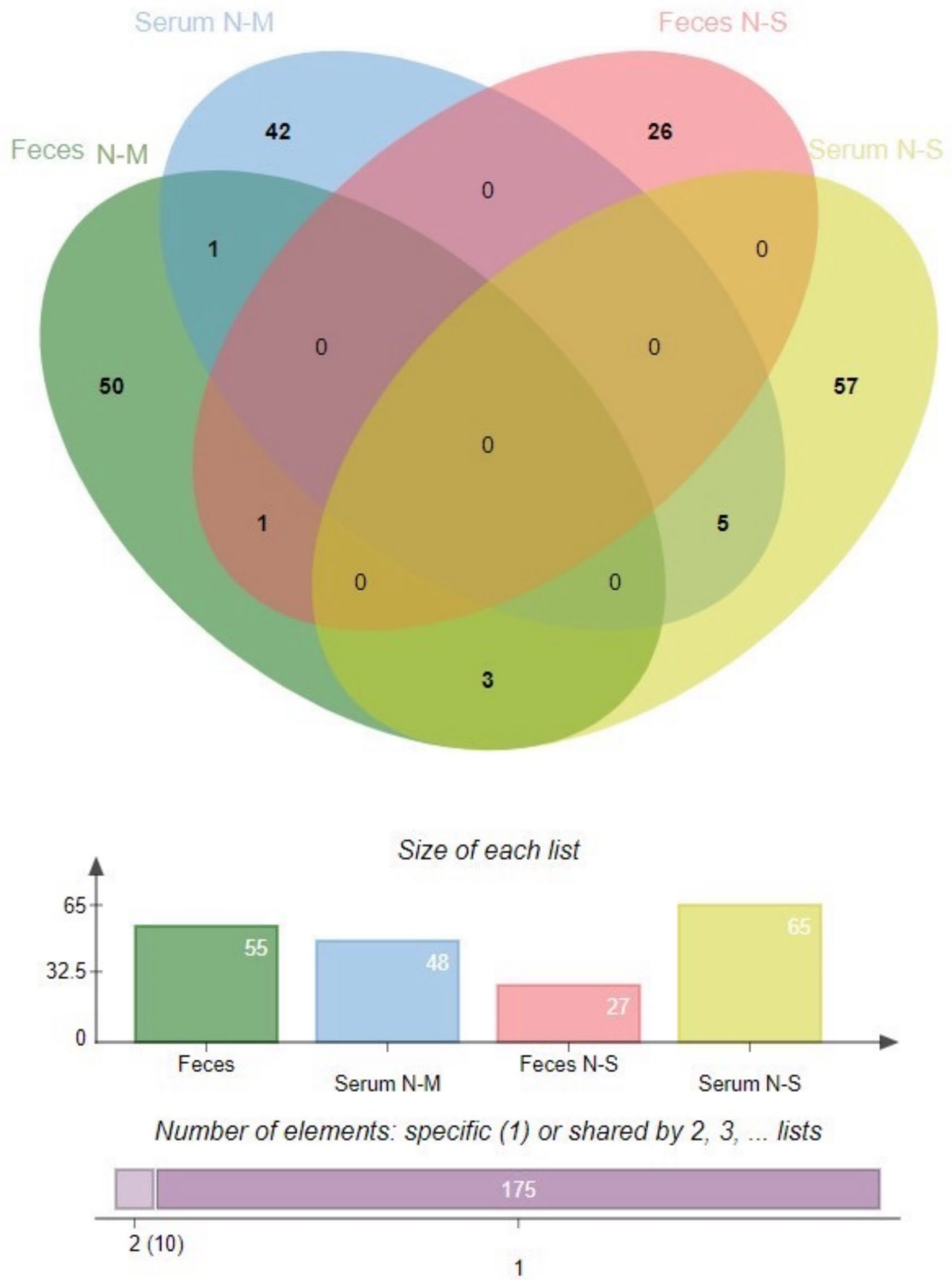


Fig. 2. Venn diagram of phosphoproteins differentially expressed in serum and fecal samples, which were aggregated using the method described¹¹. (<http://jvenn.toulouse.inra.fr/>, accessed on 13 March 2024).

alterations in lipid metabolism play a contributory role. Other factors, such as genetics, immune function, and environmental exposures, may also influence the development and progression of equine melanoma tumors.

Identification of differently expressed phosphoproteins throughout the stage of EMN

This study found that a variety of significant phosphoproteins in serum and feces of each stage of EMN, interestingly only SNW Domain Containing 1 (SNW1) protein has found in both serum and feces in the mild

Quantity and stage of phosphoprotein expression	Protein ID	Protein name	Category	Padj
1 in Serum N-M and Fecal N-M	K9KE82	SNW domain-containing protein 1 (SNW1)	Genetic information processing	< 0.01
1 in Fecal N-M and Fecal N-S	F7B680	G protein subunit alpha transducin 1 (GNAT1)	Organismal systems	< 0.01
3 in Fecal N-M and Serum N-S	A0A9L0S0L2	kinesin-like protein (KIF5B)	Cellular processes	< 0.01
	A0A9L0T2D9	protein phosphatase 4 regulatory subunit 3B (PPP4R3B)	Organismal systems	< 0.01
	A0A9L0T895	zinc finger protein 283 (ZNF283)	Human diseases	< 0.01
5 in Serum N-M and Serum N-S	F6ZPA5	Forkhead box protein N3 (FOXN3)	N/A	< 0.01
	A0A9L0R454	NADH-ubiquinone oxidoreductase 75 kDa subunit, mitochondrial(NDUFS1)	Metabolism	< 0.01
	K9K2T7	Ribokinase-like protein	Metabolism	< 0.01
	A0A9L0TQN9	Bax inhibitor 1 (TMBIM6)	Human diseases	< 0.01
	F6Q5G9	ETS variant transcription factor 2 (ETV2)	N/A	< 0.01

Table 3. List of significant phosphoproteins differentially expressed throughout EMN stages in serum and fecal samples.

EMN. G protein subunit alpha transducin 1 (GNAT1) was found in feces in both mild and severe EMN. Kinesin family member 5B (KIF5B), Protein phosphatase 4 regulatory subunit 3B (PPP4R3B) and Zinc finger protein 283 (ZNF283) were commonly found in serum of severe EMN and feces of mild EMN. Since merely SNW1 was found in both serum and feces in the mild EMN, we proposed that SNW1 might play a key role to start forming EMN in horses.

G protein subunit alpha transducin 1 (GNAT1)

GNAT1 was found in feces in both mild and severe EMN in this study. GNAT1 or transducing alpha-1 chain is involved in transmission of light signals in the retinal of the eye. Mutation in GNAT1 causes autosomal dominant congenital stationary night blindness¹⁵. It is reported as a novel melanoma-associated retinopathy antigen¹⁶. It also expresses in various human melanoma cell lines, which are induced cell differentiation by cAMP and cAMP response element-binding protein (CREB)¹⁷. Inhibition the interaction between GNAT1 and phosphodiesterase (PDE) suppresses the melanoma cells¹⁸. These findings suggest that GNAT1 regulates cGMP signaling and cell proliferation in melanoma.

Other common phosphorylated proteins

Kinesin family member 5B (KIF5B), Protein phosphatase 4 regulatory subunit 3B (PPP4R3B) and Zinc finger protein 283 (ZNF283) were found in both mild and severe EMN. KIF5B, gene encoding kinesin motor protein, acts as an intracellular carriage. KIF5B play the key role to move melanosome from the perinucleus to the peripheral cells^{19–21}. It facilitates microtubule-related melanosome transport toward the peripheral region¹⁹. Downregulation of KIF5B by miR-203 resulted in the inhibition of melanosome transport²¹. PPP4R3B is one of regulatory subunits of protein phosphatase 4 complex. The regulatory subunits of PP4 are highly conserved across mammals, yeast and plants. Binding with PPP4C, a catalytic subunit of PP4, forming the heterodimer to regulate protein dephosphorylation²². ZNF283 is belong to zinc finger protein family which functions as DNA-binding transcription factors in tumorigenesis and tumor progression²³ and immune system²⁴.

SNW1 protein and related functions and pathways associated with EMN

Following the DESeq2 test analysis, we identified a single putative phosphoprotein, SNW domain-containing protein 1 (SNW1), which was found to be expressed in both N-M of serum and N-M of fecal sample. In addition, SNW1 had the indirect with MAGED2 interaction of protein-protein interaction of *Equus caballus* as shown in Fig. 4C. Considering on interaction between SNW1 and MAGED2, the current dataset showed indirect interaction. SNW1 involved in critical biological processes, such as transcription regulation and cell proliferation, which are central to melanoma progression mediating on MAGED2-associated processes. Concerning on SNW1, it is important role since SNW1 was identified in both serum and fecal samples at the same stage which is suggested an involvement in melanoma-related processes. Moreover, DESeq2 data analysis highlights SNW1 as significantly relevant in melanoma-related pathways. Taken together, SNW1 plays a crucial biological role.

SNW Domain Containing 1 (SNW1) is also known as nuclear protein SkiP, nuclear receptor coactivator NcoA-62 or Ski interacting protein (SKIP). It restricts in the nucleus and expressed in many tissues, including brain, endocrine tissues, bone marrow and immune system, muscle, lung, liver, gall bladder, pancreas, gastrointestinal tract, kidney, urinary bladder, male and female specific tissues, adipose and skin (<https://atlasgeneticsoncology.org>). SNW1 is a transcriptional co-regulator that involved in mRNA splicing and transcription, cell cycle progression, acute and chronic inflammation responses²⁵. SNW1 has been reported that can be regulated by vitamin D, retinoic acid, estrogens, glucocorticoids, Notch1-IC and TGF- β ^{25–29}. In the recent study, only SNW1 was found in both serum and feces in mild EMN. SNW1 associated with EMN might be explained in 2 mechanisms. First, it involved directly in cell tumor proliferation because of its transcriptional property. Second, it causes chronic inflammation of EMN and induces the nuclear factor kappa B (NF- κ B) pathway. The high expression of SNW1 is reported in varieties of cancer, including hepatocellular carcinoma³⁰, bladder

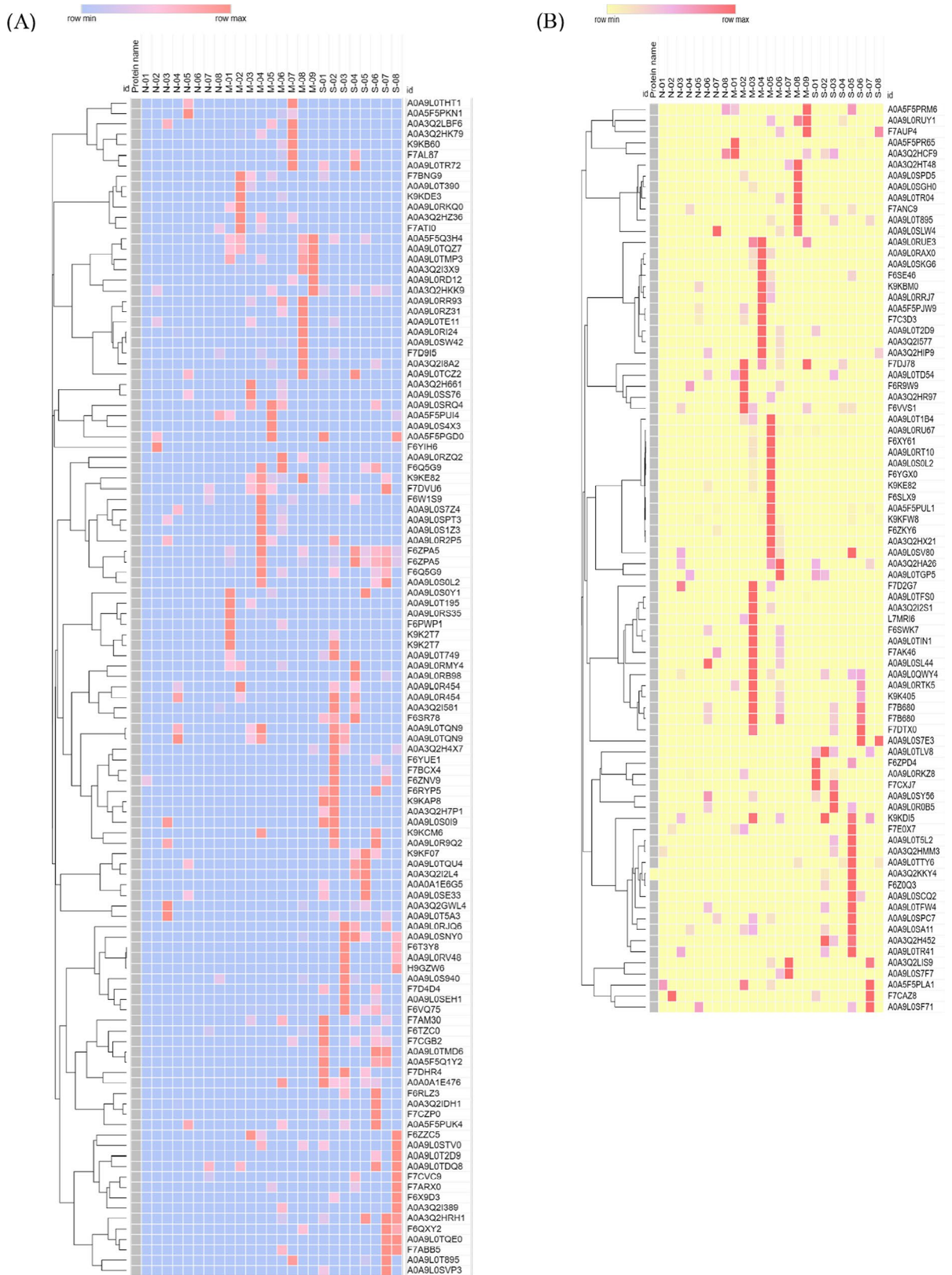


Fig. 3. Heatmaps represent the comparative of serum phosphoprotein (A) and fecal phosphoprotein (B) expression levels across a normal grey horse group, mild EMN group and severe EMN group. The heatmap was generated from the intensity of significant phosphoproteins database for each group using the CLUE program (<https://clue.io/command>, accessed on 25 March 2024), for conception. N, M and S represent normal, mild and severe, respectively.

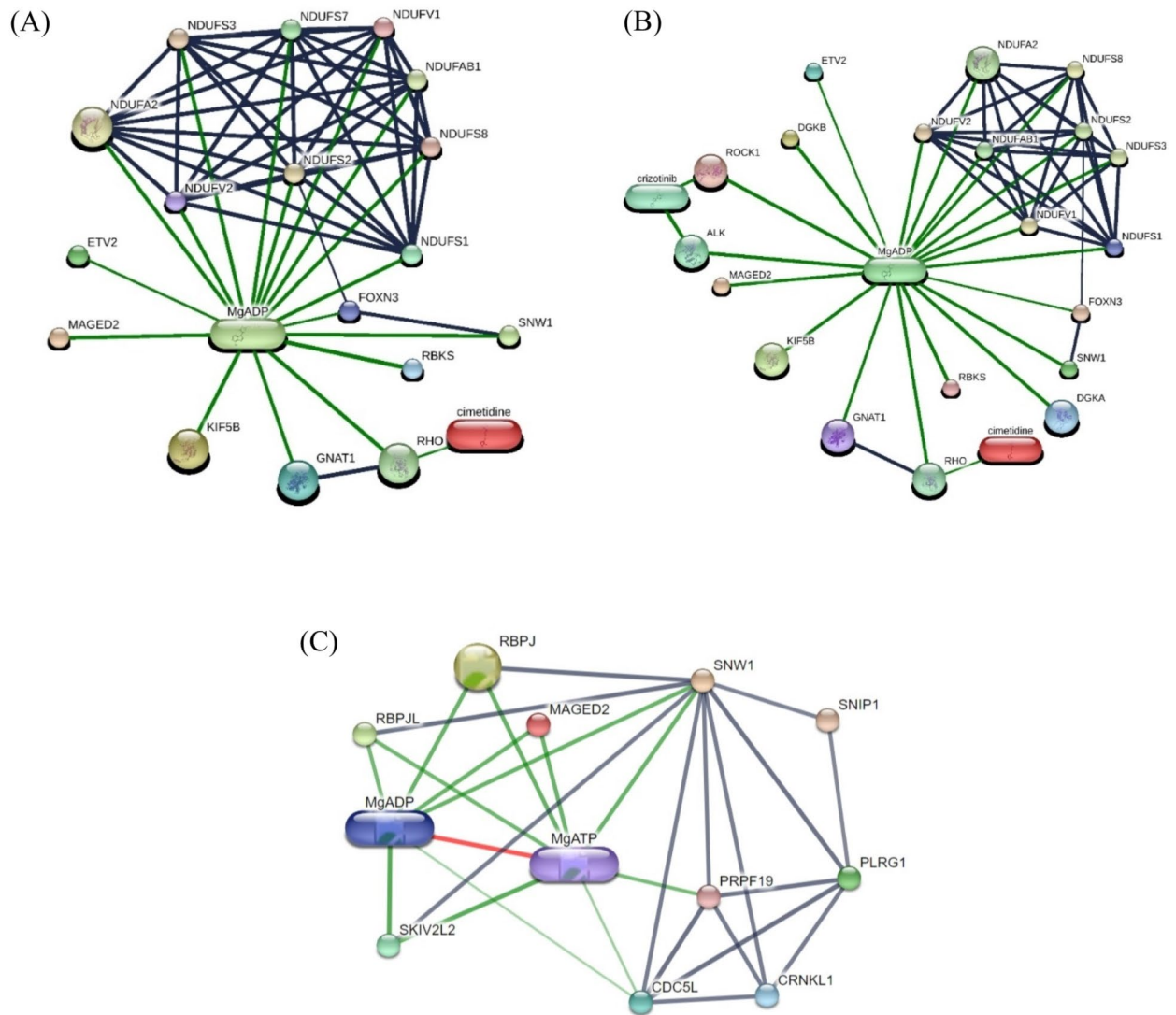


Fig. 4. The networks of the comprehensive phosphoprotein expression pattern, highlighting of notable phosphoproteins involvement (A) MAGED2 and putative of significant phosphoproteins interaction; SNW1, GNAT1, KIF5B, FOXN3, NDUFS1 and ETV2 (B) putative significant phosphoproteins and associated proteomics interaction with MAGED2; SNW1, GNAT1, KIF5B, FOXN3, NDUFS1, ETV2, ALK, DGKA, DGKB and ROCK1 (C) SNW1 and MAGED2 interaction of protein-protein interaction of *Equus caballus*. Abbreviations: SNW1; SNW domain-containing protein 1, GNAT1; G protein subunit alpha transducin 1, KIF5B; kinesin-like protein, FOXN3; Forkhead box protein N3, NDUFS1; NADH-ubiquinone oxidoreductase 75 kDa subunit, mitochondrial, ETV2; ETS variant transcription factor 2, ALK; Tyrosine-protein kinase receptor, DGKA; diacylglycerol kinase alpha, DGKB; diacylglycerol kinase beta, ROCK1; Rho-associated protein kinase and MAGED2; melanoma antigen family D2 in *Equus caballus* that computational prediction between organism and interaction aggregated by the Stitch program (www.stitch.embl.de, accessed on 13 March 2024) Version 5.0.

cancer³¹, breast cancer³², malignant pleural mesothelioma³³, and prostate cancer³⁴. Mutation of SNW1 is one of the most common gene of the splicing machinery found in melanomas³⁵, MAGE-A1, the gene encodes a human melanoma antigen, interacts with SNW1, through its C-terminal part and recruiting histone deacetylase HDAC1³⁶. SNW1 is essential for cancer cell survival, it modulates p21^{Cip1} protein expression and splicing. Inactivated SNW1 causes apoptosis of cancer cells and further induce p53 levels when works together with DNA damage agents such as UV or 5-FU³⁷. SNW1 ablation also induces apoptosis in breast cancer cells³⁸. Overexpression of SNW1 can be a prognostic marker and therapeutic target of various cancers in human, including hepatocellular carcinoma³⁰, bladder cancer³¹, breast cancer³², malignant pleural mesothelioma³³, and prostate cancer³⁴. To the best of our knowledge, there are no previous reports indicate SNW1 associated with the EMN. The recent study suggests that SNW1 might be an early detected marker for the EMN.

SNW1 is a key component to mediate the NF- κ B pathway. NF- κ B plays an important role in the process of inflammation, immune responses, cell proliferation, and biological controls in man and animals³⁹. Stimulation the NF- κ B pathway upregulates proinflammatory cytokines such as tumor necrosis factor (TNF), interleukin 6 (IL-6), interleukin 1 beta (IL-1 β) and immune cells, both B- and T-cells^{25,39}. There are 5 members involve in mammal NF- κ B family; p50, p52, p65 (RelA), RelB and c-Rel, which form homo- and heterodimeric complexes³⁹. In the classical NF- κ B pathway, p65/p50 heterodimers are typically inactive in the cytoplasm under basal stage by interacting with I κ B α . After NF- κ B is activated by proinflammatory stimuli, I κ B α is rapidly phosphorylated by IKK kinase complex causing ubiquitination-dependent degradation. Consequently, the p65/p50 complex translocate into the nucleus, and promote transcription of downstream mediators^{25,39}. To respond with stimuli such as lipopolysaccharide (LPS) and tumor necrosis factor alpha (TNF- α), NF- κ B requires SNW1 to activate its function. The mechanism that SNW1 mediates NF- κ B occurs in the nucleus. When the NF- κ B is activated, SNW1 dissociates from its splicing cofactors such as SNRNP200 and SNRNP220 and facilitates the formation of the NF- κ B-P-TEFb complex. The positive transcription elongation factor b (P-TEFb) binds to p65 stimulate the elongation of transcription by RNAPII⁴⁰ and enhancing transcriptional elongation of NF- κ B target genes; IL-6, CCL2 and COX-2³⁹. Also, P-TEFb and transcriptional elongation play key roles in cellular proliferation and cancer⁴⁰. The previous study has shown that SNW1 is always bound to P-TEFb. SNW1 also binds to its splicing cofactors, SNRNP200 and SNRNP220, during basal state³⁹. Once NF- κ B is activated by TNF- α , SNW1 dissociates from its splicing cofactors. This finding suggests that SNW1 most likely mediate NF- κ B through the regulation of transcription, not splicing. Since phosphorylated SNW1 was found in this study, we proposed that phosphorylation of SNW1 might play an important role to dissociate SNW1 and splicing cofactors. As a result, SNW1 enhances cell proliferation and differentiation in melanoma⁴¹ (Fig. 5).

Conclusions

Our study identified SNW1 in both serum and fecal samples, indicating its presence across different biological samples. As a result, this suggests that it might present as a potential biomarker. Further quantitative analysis

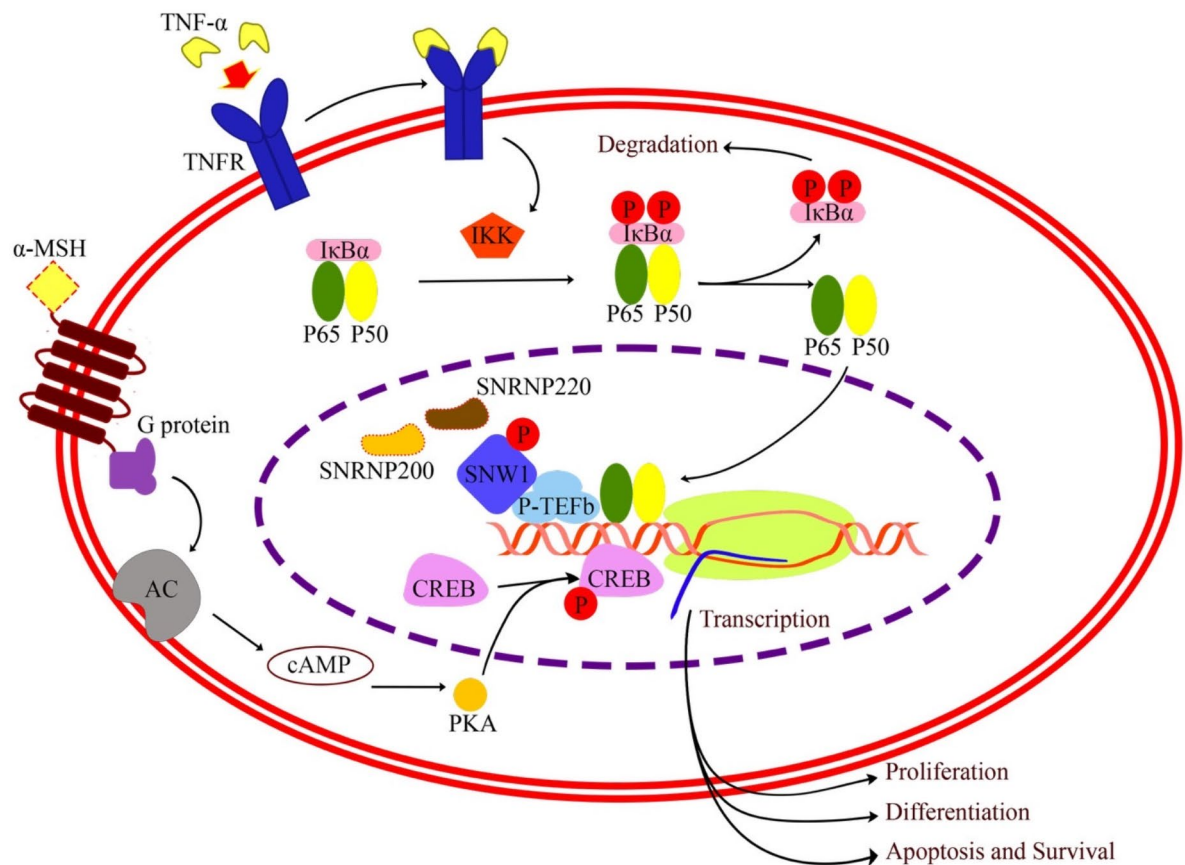


Fig. 5. Schematics of the proposed molecular pathway associated EMN (the template of molecular pathway is referred to the previous study⁴¹). Different mechanisms have been explained melanoma biology in human⁴¹. Phosphorylation of SNW1 might cause the dissociation of SNW1 and its splicing cofactors. This process facilitates the formation of the NF- κ B-P-TEFb complex³⁹. The formation of the NF- κ B-P-TEFb complex enhances transcription, proliferation and differentiation in melanoma. GNAT1 enhances cell proliferation and differentiation in melanoma via stimulation cAMP and CREB pathway¹⁷.

would be required to determine its concentration in a relation with disease progression. In a context of potential diagnostic or prognostic value, the consistent detection of SNW1 in serum and feces across different stages could be implied in the disease related biomarker. These would be required to validate the sensitivity and specificity as well. Considering clinical laboratories, ELISA or Western blotting can be recommended for further studies on antibodies for equine SNW1.

Materials and methods

Grey horses signalment

The study encompassed twenty-five grey horses, with or without appearance of melanomas. These horses represented various breeds, including Lusitano ($n=17$), Thoroughbred (TB; $n=2$), and pony ($n=6$). Among them, there was 1 stallion, 7 geldings, and 17 mares. The median age of the horses was 20 years (range, 10 to 26 years), with a median body weight of 432 kg (range, 260 to 470 kg), as detailed in Table 1. Each horse's vital signs i.e. heart rate, respiratory rate, gut sounds, mucous membrane condition, rectal temperature, and the location of melanomas, were documented. Following the classification proposed by the previous study⁴, melanomas were categorized into three groups: normal, mild, and severe EMN. In brief, horses without any melanomas were classified as the normal group or grade 0, representing healthy horses with no disease reported. Horses with nodules having a diameter of ≤ 0.5 cm were classified as the mild group or grade 1. The severe EMN group comprised horses with one or multiple nodules with a diameter exceeding 0.5 cm. This severe EMN group was further graded into 2 to 4 based on the severity of lesions, considering factors i.e. extensive confluent melanoma, exophytic tumors with moist surfaces and ulceration, and metastases in various organs.

All methods were carried out in accordance with relevant guidelines and regulation, and the study was performed in compliance with the ARRIVE guidelines. The research ethics was approved by the Faculty of Veterinary Science, Mahidol University-Institute Animal Care and Use Committee (FVS-MU-IACUC-Protocol No. MUVS-2020-12-62), Animal use license No. U1-3498-2545.

Serum and fecal samples collection, preparation and protein extraction

A total of 50 samples were collected from serum (25 samples) and feces (25 samples). For serum samples were collected from each of the horses via jugular venipuncture. The serum samples were initially placed in plain serum tubes and allowed to coagulate at 4 °C, then stored at -80 °C until analysis. After being drawn into micro-container tubes and kept in an ice box, the serum samples were precipitated with acetone at a 2:1 (v: v) ratio, incubated at -20 °C, and subsequently centrifuged at 10,000 g for 10 min to extract proteins.

Fecal samples were obtained from all horses by rectal palpation. Approximately 100 mg of feces from each grey horse was weighed and dissolved in 0.5% sodium dodecyl sulfate (SDS). The mixture was then subjected to centrifugation at 10,000 x g for 10 min. The resultant supernatant was transferred to a new microcentrifuge tube for subsequent analysis.

Serum and fecal samples measurement of protein concentration

The total protein concentration in serum and feces was determined using the Lowry assay with bovine serum albumin as a standard⁷. Each sample's protein concentration was adjusted to a final concentration of 10 g/l before being subjected to the phosphoprotein enrichment procedure (Phosphoprotein Enrichment Kit, Pierce, IL, USA). The enriched phosphoprotein was concentrated using a membrane column with a 9 kDa cut-off (Phosphoprotein Enrichment Kit, Pierce, IL, USA) and desalted using gel filtration (Thermo Scientific, Rockford, IL, USA).

In-solution digestion was used on five micrograms of protein samples. Samples were completely dissolved in 10 mM ammonium bicarbonate (AMBIC), disulfide bonds were reduced using 5 mM dithiothreitol (DTT) in 10 mM AMBIC at 60 °C for 1 h, and sulfhydryl groups were alkylated at room temperature for 45 min in the dark using 15 mM Iodoacetamide (IAA) in 10 mM AMBIC. For digestion, samples were incubated at 37 °C overnight with 50 ng/l sequencing grade trypsin (1:20 ratio) (Promega, Germany). Before injecting the digested samples into the LC-MS/MS, participants must be dried and protonated with 0.1% formic acid.

Liquid chromatography-tandem mass spectrometry (LC-MS/MS)

LC-MS/MS analysis followed the previously protocol described in⁴. The tryptic peptide samples were prepared for injection into an Ultimate3000 Nano/Capillary LC System (Thermo Scientific, UK) connected to a ZenoTOF 7600 mass spectrometer (SCIEX, Framingham, MA, USA). There were 5 μ L digests peptide which a Thermo Scientific C18 Pepmap 100 precolumn (300 μ m i.d. x 5 mm, 5 μ m, 100 Å) and separated using a Thermo Scientific Acclaim PepMap RSLC C18 analytical column (75 μ m i.D. x 15 cm, 2 μ m, 100, nanoViper) within a thermostated column oven set at 60 °C. Solvents A (0.1% formic acid in water) and B (0.1% formic acid in 80% acetonitrile) were employed with a gradient of 5–55% solvent B over 30 min at a constant flow rate of 0.30 l/min. The source and gas parameters on the ZenoTOF 7600 system were configured as follows: ion source gas 1 at 8 psi, curtain gas at 35 psi, CAD gas at 7 psi, source temperature at 200 °C, polarity set to positive, and spray voltage at 3300 V. For data-dependent acquisition (DDA), top 50 most abundant precursor ions per survey MS1 for MS/MS with an intensity threshold exceeding 150 cps were selected. Precursor ions were dynamically excluded for 12 s after two incidences of MS/MS sampling (with dynamic collision energy enabled). The MS2 spectra were collected in the range 100–1,800 m/z with a 50-ms accumulation time and Zeno trap enabled. The collision energy parameters included a declustering potential of 80 V, no DP spread, and a CE spread of 0 V. The time bins were summed (with all channels enabled) using a 150,000 cps Zeno trap threshold. The cycle time for the Top 60 DDA method was 3.0 s. Each sample underwent triplicate LC-MS analysis.

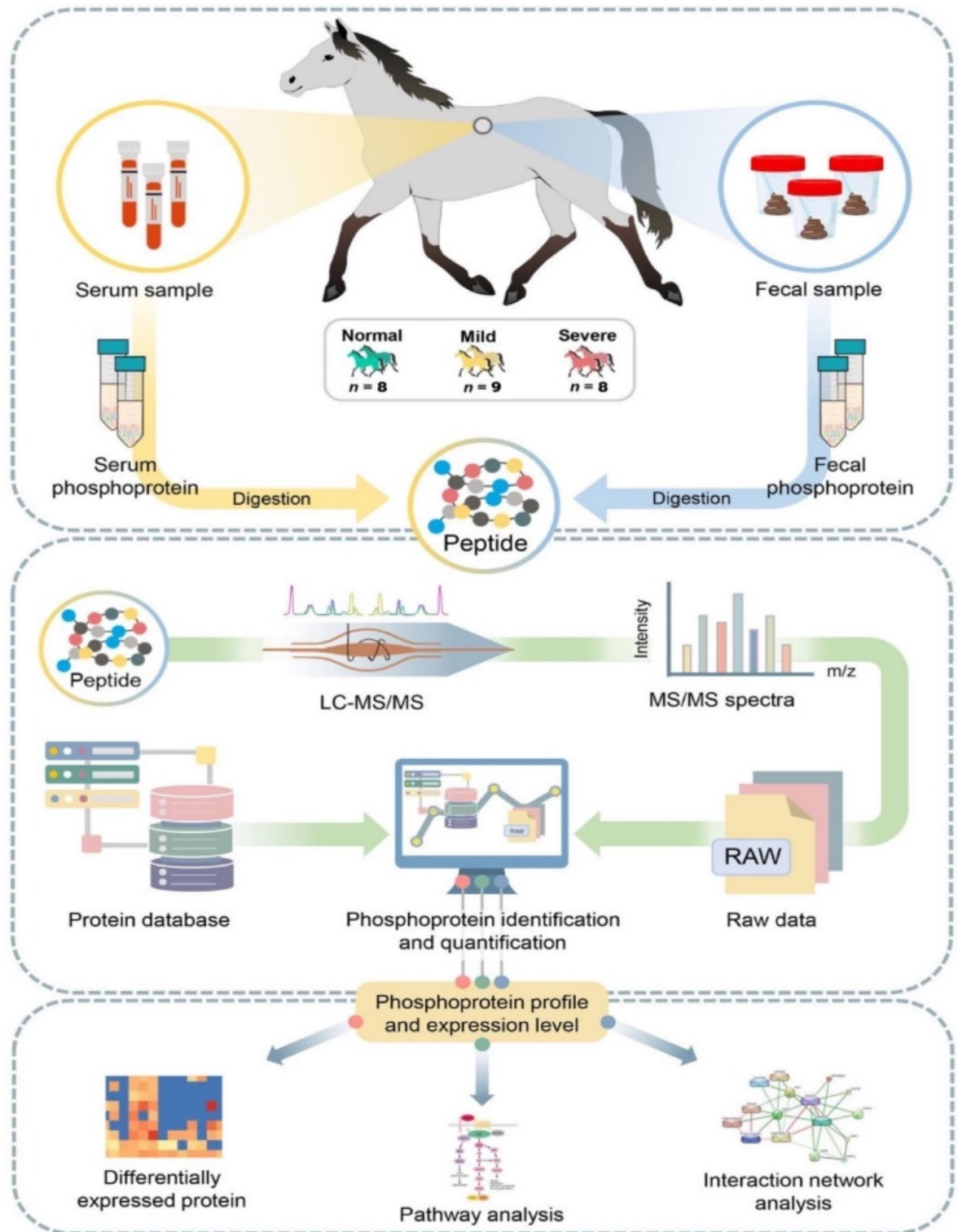


Fig. 6. Integrative workflow for phosphoproteomic profiling, DEPs analysis, pathway analysis and protein-protein interaction network.

Quantification and identification of phosphoproteins

The MaxQuant 2.4.9.0 software was used to quantify phosphoprotein in individual samples, while the Andromeda search engine was used to correlate MS/MS spectra with the Uniprot Equine database⁸. The label-free quantitation was performed using MaxQuant's standard settings, including a maximum of three missed cleavages, a mass tolerance of 0.6 dalton, trypsin as the digesting enzyme, carbamidomethylation of cysteine as a fixed modification, and oxidation of methionine as a variable modification. The peptide charge state was

also considered, with options for 1+, 2+, and 3+. The MultiExperiment Viewer (MeV) from the TM4 suite software was used for visualization and statistical analysis⁹. Maximum peptide intensities were selected to provide the protein expression levels (PELs) for DEPs analysis. The raw MS/MS spectra data are available in ProteomeXchange: JPST003099 and PXD052157.

Comparative differentially expressed phosphoproteins (DEPs) analysis towards functional annotation

The DEPs analysis was performed between EMN stage (i.e., mild and severe) and normal groups using PELs for each protein. The significant difference in phosphoproteins was examined using Wald test in DESeq2, and log₂FC was added using the lfcShrink function with ‘ashr’ adaptive shrinking. Benjamini–Hochberg correction was used for multiple testing to define differentially phosphoproteins (FDR < 0.05). For multiple testing correction, the Benjamini–Hochberg (BH)⁴² procedure was selected due to its effectiveness in controlling the false discovery rate (FDR), a key advantage in studies involving multiple comparisons. This method, commonly used in bioinformatics and omics research, balances the need to identify meaningful biological associations without an overly conservative approach, which might increase false negatives. These significant phosphoprotein expressions were considered as potential indicators for classifying EMN severity and understanding functional networks in horses. For functional annotation, The KEGG database¹⁰ was used to assign functions of the DEPs, providing KEGG Orthology (KO) IDs. The KO IDs were categorized into main and sub-function. Subsequently, a Venn diagram was used to identify uniquely or co-expressed DEPs between serum (N-M and N-S groups) and feces (N-M and N-S groups) (<http://jvenn.toulouse.inra.fr/>)¹¹.

Identification of putative protein, potential function and associated routes involved in EMN using integrative analysis

To identify putative proteins, potential metabolic function and associated routes in each stage of EMN. Here, the results obtained from phosphoproteomic and proteomic data taken from the previous study⁴ of serum and feces samples were integrated, as well as included proteins like ALK, ROCK1, DGKA, and DGKB, into STITCH to explore potential protein interactions and regulatory mechanisms influenced by phosphorylation. This integrated data allows us to explore both the known and novel roles of phosphoproteins. After analyzing DEPs and metabolic functions, the significant phosphoprotein and protein from serum and feces samples under p-adjust value < 0.05 were then considered. To construct the protein-protein interaction (PPI) networks, the STITCH database (www.stitch.embl.de)¹² was used to predict the phosphoprotein-protein-chemicals interaction involved in equine melanoma. Based on KEGG database, the targets of key proteins were mapped to pathways. Additionally, literature mining and manual curation were conducted to unveil the putative proteins (i.e., phosphoprotein and protein) and potential metabolic functions and associated routes. The framework of phosphoproteomic characterization contributing to DEP analysis and functional annotation is shown in Fig. 6.

Statistical analysis

The DEPs analysis was performed between EMN stage (i.e., mild and severe) and normal groups using PELs for each protein. The significant difference in phosphoproteins was examined using Wald test in DESeq2, and log₂FC was added using the lfcShrink function with ‘ashr’ adaptive shrinking. The Benjamini–Hochberg correction⁴², commonly used in omics analysis, was used for multiple testing to identify differentially expressed phosphoproteins (FDR < 0.05).

Data availability

The raw MS/MS spectra data are available in ProteomeXchange: JPST003099 and PXD052157. The datasets used and/or analysed during the current study are available from the corresponding author on reasonable request.

Received: 21 May 2024; Accepted: 26 November 2024

Published online: 28 December 2024

References

- Smith, S. H., Goldschmidt, M. H. & Mcmanus, P. M. A comparative review of melanocytic neoplasms. *Vet. Pathol.* **39** (2002).
- Moore, J. et al. Melanoma in horses: Current perspectives. *Equin Vet. Educ.* **25**, 144–151 (2013).
- Valentine, B. A. Equine melanocytic tumors: a retrospective study of 53 horses (1988–1991). *J. Vet. Intern. Med.* **9**, 291–297 (1995).
- Tesena, P. et al. Faecal proteomics and functional analysis of equine melanocytic neoplasm in grey horses. *Vet. Sci.* **9** (2), 94. <https://doi.org/10.3390/vetsci9020094> (2022).
- Gerritsen, J. S. & White, F. M. Phosphoproteomics: A valuable tool for uncovering molecular signaling in cancer cells. *Exp. Rev. Proteom.* **18**, 8. <https://doi.org/10.1080/14789450.2021.1976152> (2021).
- Desser, H., Niebauer, G. & Gebhart, W. Polyamin- und Histamingehalt Im Blut Von pigmentierten, depigmentierten und melanomtragenden Lipizzanerperden. *Z. f. Veterinärmedizin Reihe A.* **27**, 45–53 (1980).
- Lowry, O., Roserough, N., Farr, A. & Randall, R. Protein measurement with the folin phenol reagent. *J. Biol. Chem.* **193**, 265–275 (1951).
- Tyanova, S., Temu, T. & Cox, J. The MaxQuant computational platform for mass spectrometry-based shotgun proteomics. *Nat. Protoc.* **11** (12), 2301–2319 (2016).
- Howe, E., Sinha, R., Schlauch, D. & Quackenbush, J. RNA-Seq analysis in MeV. *Bioinformatics* **27**, 3209–3210 (2011).
- Kanehisa, M., Goto, S., Kawashima, S., Okuno, Y. & Hattori, M. The KEGG resource for deciphering the genome. *Nucleic Acids Res.* **32**, D277–D280. <https://doi.org/10.1093/nar/gkh063> (2004).
- Bardou, P., Mariette, J., Escudié, F., Djemiel, C. & Klopp, C. Jvenn: An interactive Venn diagram viewer. *BMC Bioinform.* **15**, 293. <https://doi.org/10.1186/1471-2105-15-293> (2014).
- Kuhn, M., von Mering, C., Campillos, M., Jensen, L. J. & Bork, P. STITCH: interaction networks of chemicals and proteins. *Nucl. Acids Res.* <https://doi.org/10.1093/nar/gkm795> (2008).

13. P. S., Stricker, C., Joerg, H., Dummer, R. & Stranzinger, G. A comparative genetic approach for the investigation of ageing grey horse melanoma. *J. Anim. Breed. Genet.* **117**, 73–82 (2000).
14. Pellerin, L., Carrie, L., Dufau, C., Nieto, L. & Ségui, B. LeVade, T. lipid metabolic reprogramming: Role in melanoma progression and therapeutic perspectives. *Cancers* **12**, 3147 (2020).
15. Naeem, M. A. et al. Riazuddin, S. GNAT1 associated with autosomal recessive congenital stationary night blindness. *Invest. Ophthalmol. Vis. Sci.* **53** (3). <https://doi.org/10.1167/iovs.11-8026> (2012).
16. Potter, M. J. et al. Autoantibodies to transducin in a patient with melanoma-associated retinopathy. *Am. J. Ophthalmol.* **134** (1). [https://doi.org/10.1016/S0002-9394\(02\)01431-9](https://doi.org/10.1016/S0002-9394(02)01431-9) (2002).
17. Lee, E. S., Kang, W. H., Jin, Y. H. & Juhn, Y. S. Expression of signal transducing G proteins in human melanoma cell lines. *Exp. Mol. Med.* **29** (4). <https://doi.org/10.1038/emmm.1997.34> (1997).
18. Johnston, C. A. et al. Minimal determinants for binding activated G α from the structure of a G α -peptide dimer. *Biochemistry* **45** (38), 11390–11400. <https://doi.org/10.1021/bi0613832> (2006).
19. Hara, M. et al. Kinesin participates in melanosomal movement along melanocyte dendrites. *J. Invest. Dermatol.* **114** (3). <https://doi.org/10.1046/j.1523-1747.2000.00894.x> (2000).
20. Ishida, M., Ohbayashi, N. & Fukuda, M. Rab1A regulates anterograde melanosome transport by recruiting kinesin-1 to melanosomes through interaction with SKIP. *Sci. Rep.* <https://doi.org/10.1038/srep08238> (2015). 5.
21. Noguchi, S. et al. MicroRNA-203 regulates melanosome transport and tyrosinase expression in melanoma cells by targeting kinesin superfamily protein 5b. *J. Invest. Dermatol.* **134**(2) (2014). <https://doi.org/10.1038/jid.2013.310>
22. Park, J., & Lee, D. H. Functional roles of protein phosphatase 4 in multiple aspects of cellular physiology: A friend and a foe. *In BMB Rep.* **5**(4) <https://doi.org/10.5483/BMBREP.2020.53.4.019> (2020).
23. Li, X. et al. Structures and biological functions of zinc finger proteins and their roles in hepatocellular carcinoma. *Biomark. Res.* **10** (1). <https://doi.org/10.1186/s40364-021-00345-1> (2022).
24. Rakhra, G. & Rakhra, G. Zinc finger proteins: Insights into the transcriptional and post transcriptional regulation of immune response. *Mol. Biol. Rep.* **48** (7). <https://doi.org/10.1007/s11033-021-06556-x> (2021).
25. Zhang, Q., Liang, T., Gu, S., Ye, Y. & Liu, S. SNW1 interacts with IKK γ to positively regulate antiviral innate immune responses against influenza a virus infection. *Microb. Infect.* **22** (10). <https://doi.org/10.1016/j.micinf.2020.07.009> (2020).
26. Baudino, T. A. et al. Isolation and characterization of a novel coactivator protein, NCoA-62, involved in vitamin D-mediated transcription. *J. Biol. Chem.* **273** (26). <https://doi.org/10.1074/jbc.273.26.16434> (1998).
27. Leong, G. M. et al. Ski-interacting protein interacts with smad proteins to augment transforming growth factor- β -dependent transcription. *J. Biol. Chem.* **276** (21). <https://doi.org/10.1074/jbc.M010815200> (2001).
28. Zhang, C. et al. Ternary complexes and cooperative interplay between NCoA-62/ ski-interacting protein and steroid receptor coactivators in vitamin D receptor-mediated transcription. *J. Biol. Chem.* **276** (44). <https://doi.org/10.1074/jbc.M106263200> (2001).
29. Zhou, S. et al. SKIP, a CBF1-associated protein, interacts with the ankyrin repeat domain of NotchIC to facilitate NotchIC function. *Mol. Cell. Biol.* **20** (7). <https://doi.org/10.1128/mcb.20.7.2400-2410.2000> (2000).
30. Liu, G. et al. High SKIP expression is correlated with poor prognosis and cell proliferation of hepatocellular carcinoma. *Med. Oncol.* **30** (3). <https://doi.org/10.1007/s12032-013-0537-4> (2013).
31. Wang, L. et al. SKIP expression is correlated with clinical prognosis in patients with bladder cancer. *Int. J. Clin. Exp. Pathol.* **7**(4) (2014).
32. Liu, X. et al. Expression and prognostic role of SKIP in human breast carcinoma. *J. Mol. Histol.* **45** (2). <https://doi.org/10.1007/s10735-013-9546-z> (2014).
33. Türkcü, G. et al. Comparison of SKIP expression in malignant pleural mesotheliomas with Ki-67 proliferation index and prognostic parameters. *Polish J. Pathol.* **67**(2) (2016). <https://doi.org/10.5114/pjp.2016.61445>
34. Höflmayer, D., Willich, C., Hube-Magg, C., Simon, R., Lang, D., Neubauer, E., Jacobsen, F., Hinsch, A., Luebke, A. M., Tsourlakis, M. C., Huland, H., Graefen, M., Haese, A., Heinzer, H., Minner, S., Büschel, F., Sauter, G., Schlomm, T., Steurer, S., Bernreuther, C. SNW1 is a prognostic biomarker in prostate cancer. *Diagnostic Pathol.* **14**(1) <https://doi.org/10.1186/s13000-019-0810-8> (2019).
35. Hakobyan, S., Loeffler-Wirth, H., Arakelyan, A., Binder, H. & Kunz, M. A transcriptome-wide isoform landscape of melanocytic nevi and primary melanomas identifies gene isoforms associated with malignancy. *Int. J. Mol. Sci.* **22** (13). <https://doi.org/10.3390/ijms22137165> (2021).
36. Laduron, S. et al. MAGE-A1 interacts with adaptor SKIP and the deacetylase HDAC1 to repress transcription. *Nucl. Acids Res.* **32** (14). <https://doi.org/10.1093/nar/gkh735> (2004).
37. Chen, Y., Zhang, L. & Jones, K. A. SKIP counteracts p53-mediated apoptosis via selective regulation of p21 Cip1 mRNA splicing. *Genes Dev.* **25**(7), 701–716 (2011). <https://doi.org/10.1101/gad.2002611>
38. Sato, N., Maeda, M., Sugiyama, M., Ito, S., Hyodo, T., Masuda, A., Tsunoda, N., Kokuryo, T., Hamaguchi, M., Nagino, M., & Senga, T. Inhibition of SNW1 association with spliceosomal proteins promotes apoptosis in breast cancer cells. *Cancer Med.* **4**(2), 268–277 <https://doi.org/10.1002/cam4.366> (2015).
39. Verma, S., De Jesus, P., Chanda, S. K. & Verma, I. M. SNW1, a novel transcriptional regulator of the NF- κ B pathway. *Mol. Cell. Biol.* **39** (3). <https://doi.org/10.1128/mcb.00415-18> (2019).
40. Barboric, M. et al. B., NF- κ B binds P-TEFb to stimulate transcriptional elongation by RNA polymerase II. *Mol. Cell.*, **8** (2001).
41. Eggermont, A. M. M., Spatz, A. & Robert, C. Cutaneous melanoma. *Lancet* **383** (9919), 816–827. [https://doi.org/10.1016/S0140-6736\(13\)60802-8](https://doi.org/10.1016/S0140-6736(13)60802-8) (2014).
42. Benjamini, Y. & Hochberg, Y. Controlling the false discovery rate: A practical and powerful approach to multiple testing. *J. R. Stat. Soc. Ser. B.* **57** (1), 289–300. <https://doi.org/10.1111/j.2517-6161.1995.tb02031> (1995).

Acknowledgements

This research project is supported by Mahidol University (MU's Strategic Research Fund): 2023. Functional Proteomics Technology Laboratory, National Centre for Genetic Engineering and Biotechnology (BIOTEC), Department of Clinical Science and Public Health, Faculty of Veterinary Science, Mahidol University, and Horseshoe Point International Riding School. The authors would also like to thank the Department of Zoology, the Faculty of Science, Kasetsart University, SciKU Biodata Server, Faculty of Science, Kasetsart University for resources and computing facilities.

Author contributions

Conceptualization, W. V., S. R., A. K., R. V., P. Y. and P. T.; methodology, P. T., A. K., W. V., N. P. and S. R.; investigation, P. T., A. K., W. V., N. P. and S. R.; resources, P. T., A. K., W. V., N. P. and S. R.; data curation, P. T., A. K., W. V., N. P. and S. R.; writing original draft preparation, R. V., A. K., and P. T.; writing, review and editing, P. T., R. V., A. K., W. V., N. P., S. R., P. Y. and P. T.; project administration, W. V. and P. T.; funding acquisition, W. V. and P. T., All authors have read and agreed to the published version of the manuscript.

Funding

This research project is supported by Mahidol University (MU's Strategic Research Fund): 2023.

Declarations

Competing interests

The authors declare no competing interests.

Ethics approval

All methods were carried out in accordance with relevant guidelines and regulation, and the study was performed in compliance with the ARRIVE guidelines. The research ethics was approved by the Faculty of Veterinary Science, Mahidol University-Institute Animal Care and Use Committee (FVS-MU-IACUC-Protocol No. MUVS-2020-12-62), Animal use license No. U1-3498-2545.

Additional information

Supplementary Information The online version contains supplementary material available at <https://doi.org/10.1038/s41598-024-81338-6>.

Correspondence and requests for materials should be addressed to W.V. or P.T.

Reprints and permissions information is available at www.nature.com/reprints.

Publisher's note Springer Nature remains neutral with regard to jurisdictional claims in published maps and institutional affiliations.

Open Access This article is licensed under a Creative Commons Attribution-NonCommercial-NoDerivatives 4.0 International License, which permits any non-commercial use, sharing, distribution and reproduction in any medium or format, as long as you give appropriate credit to the original author(s) and the source, provide a link to the Creative Commons licence, and indicate if you modified the licensed material. You do not have permission under this licence to share adapted material derived from this article or parts of it. The images or other third party material in this article are included in the article's Creative Commons licence, unless indicated otherwise in a credit line to the material. If material is not included in the article's Creative Commons licence and your intended use is not permitted by statutory regulation or exceeds the permitted use, you will need to obtain permission directly from the copyright holder. To view a copy of this licence, visit <http://creativecommons.org/licenses/by-nc-nd/4.0/>.

© The Author(s) 2024